SUPPLEMENTAL MATERIAL

Savalli et al., http://www.jgp.org/cgi/content/full/jgp.201611586/DC1

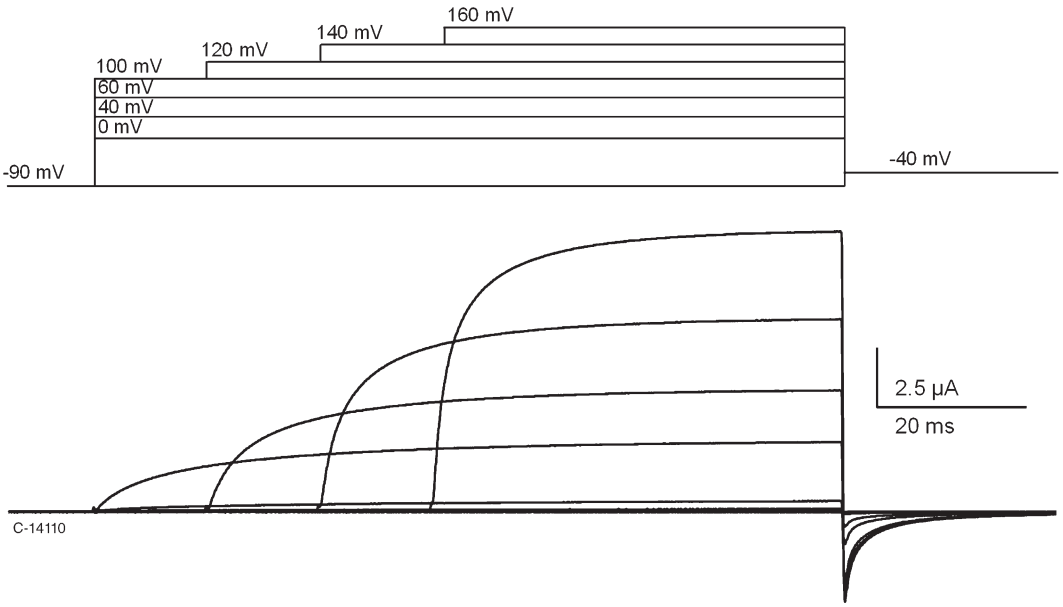

Figure S1. **Representative Ba^{2+} current traces from *Xenopus* oocytes expressing $Ca_V1.2$ channel complexes formed by α_{1C} + β_3 subunits.** Because in the absence of $\alpha_2\delta$-1 subunits the $Ca_v1.2$ channel is slow to activate, incrementally longer pulses were used to achieve quasi–steady state. The tail currents at −40 mV were used to construct the G(V) curves in Fig. 2 (black squares). The voltage protocol is reported above the current traces.

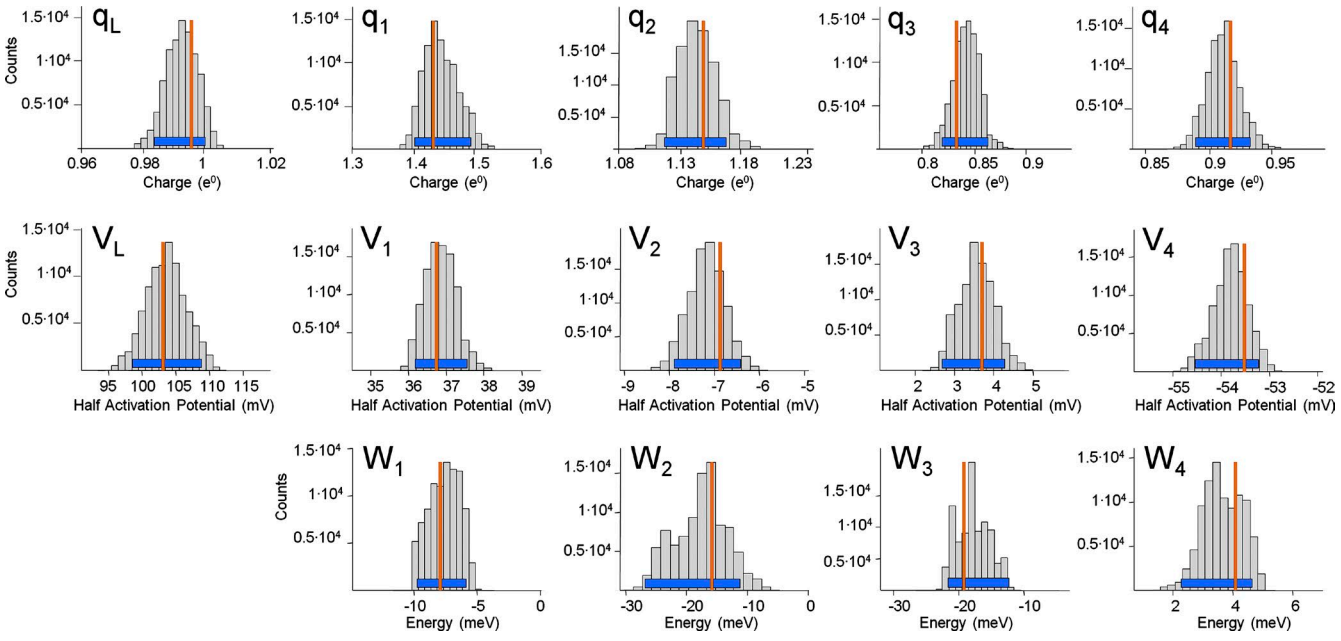

Figure S2. **Histograms of posterior distributions of 14 parameters obtained from a 100,000-trial MCMC run.** The first 6,000 values corresponding to the burn-in period that precedes the stationary phase were excluded. The orange vertical lines correspond to parameter values of the best fit that was used to generate the model predictions for fluorescence and ionic current (Fig. 6, black continuous lines). Horizontal blue bars show the 95% credible intervals that include 95% of the acceptable values visited during our statistical analysis. The bin size was scaled to maintain the most frequent value at ∼15,000 to highlight the overall similarity in shape. Histograms for the remaining 10 parameters (x_i and ν_i) are summarized in Fig. S3.

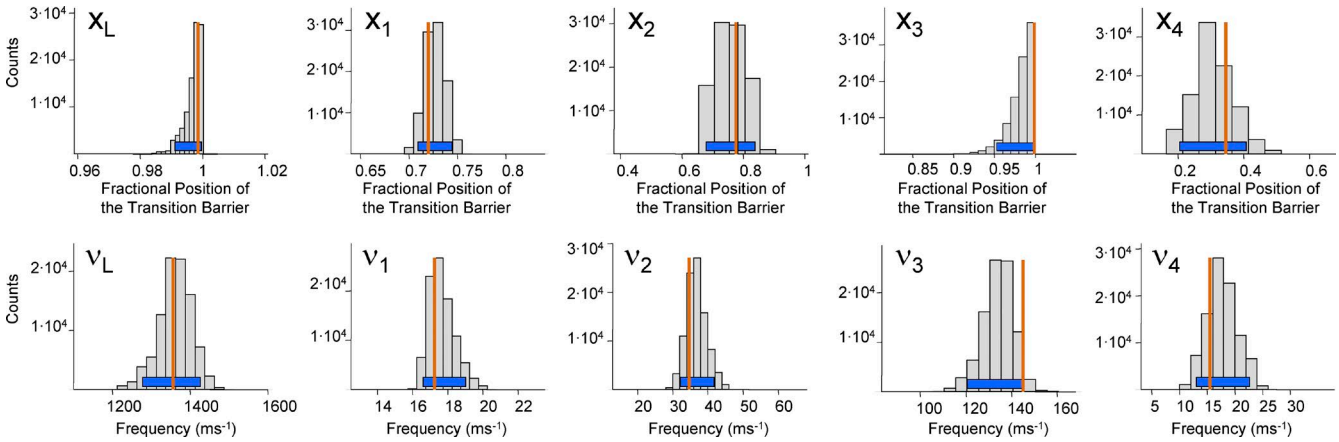

Figure S3. **Histograms of posterior distributions of parameters *xi* and *νi* (*i* = L,1,2,3,4).** As in Fig. S2, the orange vertical line corresponds to parameter values of the best fit, and the horizontal blue bars show the 95% credible interval. The bin size was scaled to maintain the most frequent value at ~25,000. To constrain the possible solutions, we added several constrains to the error function using the following equation:

$$Cstr(i) = a_i \left[\exp\left(\frac{[f(x) - f(c_i)]^2}{b_i} \right) - 1 \right],$$

where a_i is a scaling factor, b_i sets the limits of the constrains, and c_i corresponds to the optimum value. We constrained the time constants for the onset of ionic currents and fluorescence traces at 20 mV to the mean time constant obtained from single exponential fit (τ_{avg} in Table 1). We also penalized the time constant of the ionic tail current with a target value of 0.9 ms. The off relaxation of VSD II and VSD III fluorescence traces at 40 mV were also limited to 8.5 ± 2 and 8 ± 2 ms, which correspond to the time constants of the single exponential that best described the decay of the traces. Parameter sets that yielded ionic currents displaying inactivation (negative ratio between peak current and the amplitude at the end of the pulse) or with slope of ln(GV) −160 mV diverging from q_L were also penalized.